Independent Estimation of Aircraft Positions Using Space-Based ADS-B Data for GNSS Anomaly Identification and Investigation

Dr. Giuseppe Sirigu
Systems Engineering
Aireon LLC
McLean, VA, USA
giuseppe.sirigu@aireon.com

John Dolan
Systems Engineering
Aireon LLC
McLean, VA, USA
john.dolan@aireon.com

Dr. Michael A. Garcia
Systems Engineering
Aireon LLC
McLean, VA, USA
michael.garcia@aireon.com

***Abstract* — The aviation industry has been relying more and more on the availability and accuracy of Global Navigation Satellite System (GNSS) position reports to perform some of its vital functions, like aircraft separation, terrain avoidance, and flow management. The increasing occurrence of GNSS interference recorded in recent years, both intentional and unintentional, has raised safety concerns among the aviation stakeholders and it has spurred a wave of research for tools that can help identify, understand, and mitigate these events and their impact on flight operations. Aireon, by exploiting the unique features of its system, has developed a global independent position estimator, RefTrack, with the purpose of providing a reliable source of information about the location of aircraft when GNSS position reports are not trustworthy. The generated position estimations can be used to fill gaps in aircraft tracks due to the loss of GNSS positions, or to identify GNSS interference hotspots by comparing the estimated tracks against the reported ones.**

Keywords—GNSS Anomalies, Position Estimation, ADS-B, Jamming, Spoofing, Tracker, Kalman filter

I. INTRODUCTION

In the past two years, a significant increase in the number of Global Navigation Satellite System (GNSS) anomalies has been recorded at a global scale, accelerated by shifts in the global geopolitical landscape [1][2]. These anomalies can affect aircraft surveillance systems based on GNSS reports, like Automatic Dependent Surveillance-Broadcast (ADS-B) systems, posing challenges to the safety and the efficiency of operations in the aerospace industry [3].

GNSS interference can manifest itself in different ways aboard an airplane. Interference can result in significant errors in navigation positions and abnormal differences between ground speed and true airspeed. In addition, in the worst cases of spoofing, the timing aboard the aircraft has been affected, which causes not only position shifts but also the loss of internet aboard and the related services, like the collection of weather information. Finally, pilots have reported spurious terrain awareness and warning system (TAWS) alerts; these are due to shifted GNSS altitude and are particularly challenging, as they can cause unnecessary maneuvers and lower the trust of pilots on their systems [3].

Generally, the GNSS interference is localized in specific hotspot regions, like the Baltic area, Middle-East region, South-East Asia, and the Black Sea. However, the effects of this interference can continue to impact the aircraft beyond the region where it originally occurred. For example, the aircraft may experience degraded position integrity or shifted position for the remainder of the flight; in the worst cases, the GNSS cannot be rebooted while airborne.

Aireon has developed an algorithm able to independently estimate the aircraft position, based on the reception of raw ADS-B messages by multiple payloads in the Aireon system, which is an evolution of the algorithm presented in "Aireon independent validation of aircraft position via space-based ADS-B" [4]. The proposed algorithm utilizes Kalman filters [5] to track the position and offers an innovative concept in which the propagated position is used as additional measurement for Time Difference of Arrival (TDOA) computations, enabling the use of two or more receivers, in contrast to classical multilateration algorithms that require at least three receivers [6][7][8][9]. The output of Aireon's independent position estimation can be used to identify occurrences of GNSS interference [10] and improve the situational awareness of an air traffic stakeholder by providing the most likely position of an aircraft when the ADS-B reported GNSS position is not reliable.

This paper provides an overview of the Aireon system (II), highlighting its unique features that enable the computations required to estimate the position. A detailed description of the proposed algorithm is provided in III, with particular focus on the innovative technique which allows to perform TDOA computations using at least two receivers. The algorithm is still in prototype phase and results are preliminary; the authors expect that performance can greatly improve following fine-tuning of parameters, specialization to specific trajectory phases, and general improvements to the underlying logic. The current performance of the algorithm on a synthetic dataset is meant to stress-test the algorithm is analyzed in IV, whereas, the algorithm is applied to real cases of GNSS interference in Fig. 6 and in VI it is applied to one hour of traffic around the Baku (UBBA) Flight Information Region (FIR), which is an area where GNSS interference is often recorded.

II. AIREON SYSTEM

In April of 2019, the Aireon Space-Based ADS-B system went operational and began providing service to air navigation service providers around the world. The Aireon system leverages the Iridium constellation of satellites. Iridium's low-latency, 66 cross-linked Low-Earth Orbit (LEO) satellites – plus 14 orbiting spares – orbit approximately 485 miles above the earth, with each satellite linked to up to four others, creating a dynamic mesh network to ensure continuous availability, everywhere on the planet. The Iridium satellites host the Aireon ADS-B receivers that relay signals from ADS-B equipped aircraft to the ground in real-time (Fig. 1) [11].

The latency of the Aireon system amounts to less than 400ms when delivering ADS-B messages from reception at the satellite to the downstream user [12], providing a high rate of detection in many environments around the world. Although the system has a target of meeting an update interval

of 8s or less 96% of the time, it can achieve a median update rate of 2 seconds in areas with low traffic density and low interference in the 1090MHz spectrum [13].

Fig. 1. Aireon system.

III. Independent Position Estimator

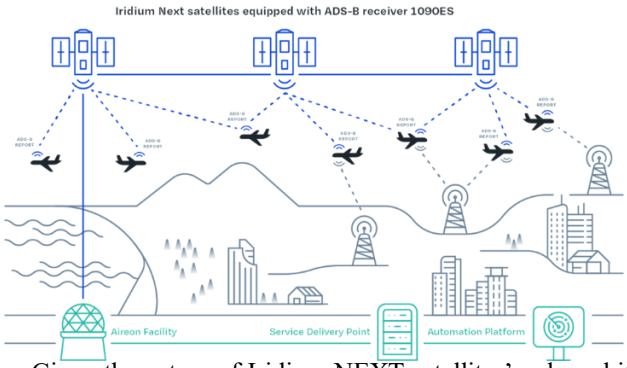

Given the nature of Iridium NEXT satellites' polar orbits and the size of Aireon payloads' footprints, all aircraft flying above 43° and below -43° latitude are always covered by at least two satellites, while near the equator the probability of footprint overlapping for an aircraft is 80%. Aireon leveraged this exclusive feature of its Space-Based ADS-B system to develop RefTrack, an independent aircraft position estimator.

The proposed algorithm uses a combination of TDOA and kinematic calculations to provide a realistic estimate of the aircraft's position globally. TDOA computations using moving receivers require highly accurate position and timing information, which Aireon receives from Iridium, thereby enabling RefTrack to exploit the several opportunities for TDOA guaranteed by the overlapping of the payload footprints.

Fig. 2. RefTrack data flow diagram.

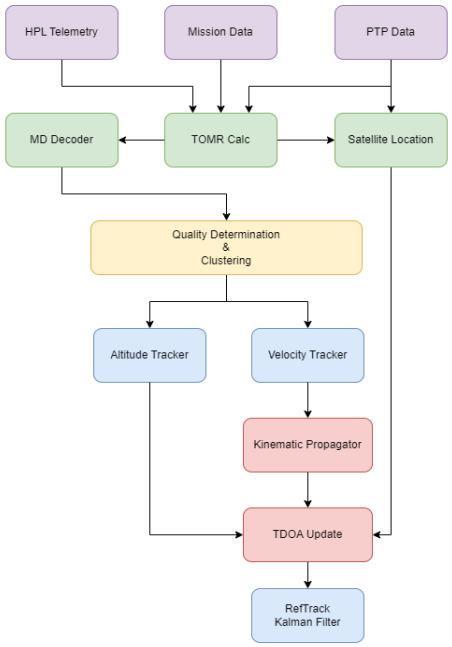

The data flow diagram depicted in Fig. 2 provides a view of the RefTrack algorithm from input to estimated positions. The remainder of this section describes in detail each portion of the algorithm.

A. *Data Gathering (Purple Boxes)*

Three sets of input data are required by the algorithm to support the necessary functions for position estimation and tracking:

- Mission Data: These are the raw ADS-B messages broadcasted by the aircraft and collected by Aireon's receivers.
- HPL Telemetry: The Hosted Payload (HPL) Telemetry messages include status information about the payload and crucial information to determine the UTC Time of Message Reception (TOMR) of each ADS-B Message.
- PTP Data: The Precision Timing and Position (PTP) Data is generated by Iridium in the PTP Controller (PTPC). This application sends the data to the Hosted Payload Operations Center (HPOC), which then delivers the data to Aireon Processing and Distribution (APD). The PTP data contain high accuracy timing correction information and position information used to support the TDOA measurements.

B. *Initial Processing (Green Boxes)*

These functions extract relevant information from the input data, such as high accuracy satellite positions and timing. Furthermore, the mission data are decoded to extract position and velocity information, following the ADS-B Minimum Operational Performance Standard (MOPS) [14].

C. *Metadata Extraction (Yellow Boxes)*

The metadata extraction steps mine extra information from the messages using multiple messages and some hysteresis. These are derived parameters that are not explicitly contained within the messages, so they require some additional processing.

1) Position and Velocity Accuracy: This function sets the accuracy for position and velocity in meters and meters per second from the reported ones, which are defined as integer values. The equations for conversion are:

$$\sigma_\pi = (\text{EPU} - 1) / 2.4477 \quad (1)$$

$$\sigma_\pi = (\text{HVE} - 0.1) / 2.4477 \quad (2)$$

Where EPU is the Estimated Position Uncertainty threshold defined as the mapping from the Navigation Accuracy Category for the position (NACp) to a value in meters from Table 2-70 in DO-260B and HVE is the Horizontal Velocity Error threshold defined as the mapping from the Navigation Accuracy Category for the velocity (NACv) to a value in meters per second from Table 2-22 in DO-260B [14]. NACp and NACv are defined as 95th percentile containments for a 2 degree of freedom (circular) distribution. The CDF for a Rayleigh distribution at the 95th percentile is ~5.99146, square root of that value is ~2.4477.

2) Bad Position Type: The bad position type check is simply looking at the ADS-B message type code to determine if there is an indication of GPS issues. Observations of real-world GPS spoofing events show a preceding drop in reported GPS quality followed by the period of spoofing where the GPS quality is reported as good. To combat this, the function tracks, through incrementing a simple counter, when an ADS-B message is any of the following:

- Type code 0.

- Type code 22.
- Position message AND type code $\geqslant$ configurable bad position threshold

3) Good Position Type: The good position type check is the inverse of the previous check and works on similar logic. Once the aircraft is no longer experiencing GPS issues we want to trust the ADS-B data once again. To do so we increment another counter whenever we receive an ADS-B message that shows all of these characteristics:

- Type code $\geqslant$ 5.
- Type code < configurable bad position threshold
- Has Compact Position Report (CPR) position data that was successfully decoded.

4) Clustering: The TDOA measurements are performed using clusters of ADS-B messages, that is, a single transmitted message received on multiple payloads. This function identifies and groups those clusters together into single entities for the downstream functions to work on them. The clusters can vary in size from 1 to 12 or more ADS-B messages, depending on the latitude of the aircraft. The clustering logic is very simple; it looks for any ADS-B messages that meet the following criteria and puts them together into a cluster:

- Received on different satellites. The purpose of the TDOA measurement is to use the geometry between the different receivers and the transmitter to independently determine an estimate of the truth position.
- Have been received within 300ms of each other. Because this application works in real-time, a cluster can only be open for so long before processing has to proceed. This gives enough time for most messages to be captured.
- TOMR difference of less than 25ms. To ensure that the messages are from the same transmission, they must have been received at the satellites in very quick succession.
- Have identical ADS-B message squitter information.

D. Trackers (Blue Boxes)

At the core of the RefTrack algorithm there are three trackers, which are based on Kalman filters. The trackers are used both to smooth data and to calculate the best estimate for values used in the processing.

The track is initialized using ADS-B data, if available, from the clusters defined at the previous step. The initialized track is then passed to the three trackers defined in this section and to the TDOA estimation functions (Section E). If no reported position information is available in the first 10 minutes of a new track, the track is initialized with position at the reference system center, defined in this instance as the projection on the Earth surface of the position of one of the satellites in view of the target (taken randomly). In this case, a warmup period is initialized, in which the track is updated but not passed in output; the warmup period ends when both of the following conditions are met:

- At least 7 minutes have elapsed.
- The velocity is lower than 309 m/s.

Velocity Tracker: The scope of this tracker is to smooth the reported velocity and to provide estimates of the velocity when the aircraft reports untrustworthy parameters or no velocity data, like during GNSS interference events. For this Kalman filter, the state vector $\mathbf{x}_{00}$ is populated with the track's velocity position x_{vel} and y_{vel} and the velocity values v_x and v_y, defined in the East North Up (ENU) reference system. In the velocity tracker the measurement, $\mathbf{y}_{00}$, and measurement covariance matrix, $\mathbf{R}$, are built from components of the overall track position information and the reported velocity data. $\mathbf{y}_{00}$ contains the track position x_{trk} and y_{trk} and the reported velocity v_{adsbx} and v_{adsby}. The prediction and update steps of this tracker follow the classical Kalman filter process.

1) Altitude Tracker: Similarly to the velocity tracker, this Kalman filter keeps accurate estimates of the altitude values used in the processing. In this case, the state vector is composed by the track's altitude, alt, and vertical rate, v_z. The measurement vector contains only the smoothed altitude, alt. Similar to the velocity tracker, the altitude tracker also follows the same equations as a classical Kalman filter.

2) RefTrack Kalman Filter: The final Kalman filter is used to smooth the outputs of the previous trackers and the TDOA estimator functions to remove jitters that can arise while infering the parameters. The state vector is populated with the output's position and velocity values x_{out}, y_{out}, v_{outx}, and v_{outy}. For this tracker, the measurements are only positon data x_{trk} and y_{trk}.

E. TDOA Estimator (Red Boxes)

A unique feature of the proposed RefTrack algorithm is the ability to update the track using TDOA measurements from two or more satellites, in contrast to classical multilateration techniques that require three or more receivers to compute TDOA measurements. This characteristic allows the application of this algorithm to regions where there is overlap of only two footprints of Aireon's payloads. This augmented capability is enabled by the use of the estimated track position as additional observation. The TDOA estimator is based on a modified Kalman filter where extra steps are taken in between the predict (the Kinematic propagator in Fig. 1) and update phases (the TDOA update in Fig. 1).

1) Kinematic Propagator: The Kinematic propagator is equivalent to a classical Kalman filter predict step where the state vector is composed of the track positon and velocity x_{trk}, y_{trk}, v_{trkx}, and v_{trky}. If the measurement is not a TDOA measurement, the outputs of the Kinematic propagator will be used to update the track position with no further calculations.

2) TDOA Update: The TDOA update function is the main differentiator between other trackers and the solution proposed in this paper. The use of TDOA measurement allows for better understanding of the real position of the aircraft when the reported position cannot be trusted, such as in cases of GNSS interference. Additional steps are performed to convert TDOA measurements into position updates. First of all, when a candidate cluster for TDOA is ingested, a sanity check is applied to verify the health of the information provided by each satellite; three conditions must be met:

a) Time Accuracy: The PTP data contains the satellite's timing accuracy; if this value is above 67ns then

the satellite's timing is too inaccurate and cannot be used for TDOA measurements.

b) Position Accuracy: The PTP data provides a full 3x3 covariance matrix to describe the satellite's position accuracy; if the square-root of the trace of this matrix is greater than 240m, then the satellite's position is too inaccurate and cannot be used for TDOA measurements.

c) Elevation Angle: If the elevation angle between the aircraft and the satellite is below -1°, the satellite should not be used for TDOA measurements, as the measurement could be impacted by refraction and/or multipath.

After removing all messages that do not pass the check above, the direction cosine matrix D, which represents the orientation of the propagated position with respect to the satellites, can be computed as follows:

$$\boldsymbol{R} = \begin{bmatrix} x_{trk} & y_{trk} & z_{trk} \\ & \vdots & \\ x_{trk} & y_{trk} & z_{trk} \end{bmatrix}_{ECEF} - \begin{bmatrix} x_{sat_1} & y_{sat_1} & z_{sat_1} \\ & \vdots & \\ x_{sat_N} & y_{sat_N} & z_{sat_N} \end{bmatrix}_{ECEF} \tag{3}$$

$$\boldsymbol{D} = \begin{bmatrix} \widehat{\boldsymbol{R}_{1:}} \\ \vdots \\ \widehat{\boldsymbol{R}_{N:}} \end{bmatrix} = \begin{bmatrix} \boldsymbol{D}_1 \\ \vdots \\ \boldsymbol{D}_N \end{bmatrix} \tag{4}$$

Where the subscript with a colon represents evaluating on the entire row vector and the "^" represents normalizing said vector. Subsequently, **z** values, representing the delta between pseudo-range and range, with the pseudo-range being the range calculated by multiplying the time difference and the speed of light c and the range **r** being the reported distance between aircraft and satellite, are computed as follows:

$$\boldsymbol{TDOA} = c \begin{bmatrix} TOMR_2 - TOMR_1 \\ \vdots \\ TOMR_N - TOMR_1 \end{bmatrix} \tag{5}$$

$$\boldsymbol{r} = \begin{bmatrix} |\boldsymbol{R}_{1:}| \\ \vdots \\ |\boldsymbol{R}_{N:}| \end{bmatrix} \tag{6}$$

$$\boldsymbol{z} = \boldsymbol{TDOA} - \begin{bmatrix} r_2 - r_1 \\ \vdots \\ r_N - r_1 \end{bmatrix} \tag{7}$$

The z values are then compared against two thresholds:

- While the reported data is trusted, the z-values are compared to a z-threshold. If any of the z-values are greater than this z-threshold, the TDOA measurement is rejected, and the reference track is updated using the prediction value.
- If the z-values are greater than the z-threshold, they are also compared to a larger threshold, the big-z-threshold. This is used to determine if the reported position is very far from the reference track. If any of the z-values are greater than big-z-threshold for a certain number of clusters, the track is set to the no trust state.

For small z-values, the observation matrix **H** can be extracted from the TDOA measurements while, at the same time, the reference is changed from the Earth-Centered Earth-Fixed (ECEF) to the ENU reference system.

$$\boldsymbol{TDOA} \cong \begin{bmatrix} r_2 - r_1 \\ \vdots \\ r_N - r_1 \end{bmatrix} = \begin{bmatrix} \boldsymbol{D}_2 - \boldsymbol{D}_1 \\ \vdots \\ \boldsymbol{D}_N - \boldsymbol{D}_1 \end{bmatrix} \Delta \boldsymbol{x}_{ECEF} = \begin{bmatrix} \boldsymbol{D}_2 - \boldsymbol{D}_1 \\ \vdots \\ \boldsymbol{D}_N - \boldsymbol{D}_1 \end{bmatrix} \boldsymbol{T} \Delta \boldsymbol{x}_{ENU} \tag{8}$$

$$\boldsymbol{H} = \begin{bmatrix} \boldsymbol{D}_2 - \boldsymbol{D}_1 \\ \vdots \\ \boldsymbol{D}_N - \boldsymbol{D}_1 \end{bmatrix} \boldsymbol{T} \tag{9}$$

With **T** being the reference system rotation matrix trimmed to consider only rotations to the East and North coordinates, as it is assumed that the altitude will be provided by the altitude tracker in the Up coordinate. The measurement covariance is calculated by combining all our known measurement errors that impact our TDOA measurement.

- Satellite Timing Error
- Satellite Position Error
- Predicted Track Position Covariance

$$\boldsymbol{R} = \begin{bmatrix} c^2\sigma_{t_2} + \boldsymbol{D}_2(\boldsymbol{T}\boldsymbol{P}_{pos}\boldsymbol{T}^T + \boldsymbol{R}_{pos_2})\boldsymbol{D}_2^T & 0 & 0 \\ 0 & \ddots & 0 \\ 0 & 0 & c^2\sigma_{t_N} + \boldsymbol{D}_N(\boldsymbol{T}\boldsymbol{P}_{pos}\boldsymbol{T}^T + \boldsymbol{R}_{pos_N})\boldsymbol{D}_N^T \end{bmatrix} + \left(c^2\sigma_{t_1} + \boldsymbol{D}_1(\boldsymbol{T}\boldsymbol{P}_{pos}\boldsymbol{T}^T + \boldsymbol{R}_{pos_1})\boldsymbol{D}_1^T\right) \tag{10}$$

Where c is the speed of light, σ_t is the satellite timing accuracy, $\boldsymbol{P}_{pos}$ is the upper-left 2x2 portion of the track covariance (the position covariance components), and $\boldsymbol{R}_{pos}$ is the satellite position covariance matrix.
Finally, the Kalman gain can be calculated using the classical equations for the tracker. The Kalman update also follows similar principles to the classical implementation, with some variations in the covariance update:

$$\mathbf{x_{11}} = \mathbf{x}_{10} + \boldsymbol{K}\cdot\boldsymbol{z} \tag{11}$$

$$\boldsymbol{P}_{11} = \begin{bmatrix} (\boldsymbol{I} - \boldsymbol{K}\boldsymbol{H})\boldsymbol{P}_{10}^{UL} & \boldsymbol{Z} \\ \boldsymbol{Z} & \boldsymbol{P}_{10}^{LR} \end{bmatrix} \tag{12}$$

Where the $\mathbf{x_{10}}$ values are the predicted track positions in the ENU coordinate frame, the UL and LR superscripts indicate the upper-left and lower-right 2x2 matrix within the covariance matrix, and the **Z** represents a 2x2 zero matrix.

Finally, the output of the tracker is converted from ENU reference to geodesic latitude, longitude, altitude (LLA) reference frame and stored in the reference track for output and future updates.

IV. Results

This section presents results of a performance analysis that was carried out on a synthetic dataset created to test the adaptability of the proposed algorithm to different realistic situations.

A. Test Case Definition

To stress test the proposed logic, a set of synthetic scenarios was created to simulate variability in the type of motion and progressive loss of position data, which happens

in cases of GNSS interference. The considered set of motion types are described in TABLE I.

TABLE I. DECRIPTION OF THE TYPES OF MOTION ANALYZED

ID	Motion Type
1	180 degrees turn
2	90 degrees turn
3	Acceleration/deceleration on straight flight
4	Climb/descent on straight flight
5	Holding patterns
6	S-curve
7	Straight line level flight

In addition, the percentage of missing position information (Coasting %) was defined between 0% and 100% of the trajectory for a given target; finally the loss of position could start at the beginning of the trajectory (value 1) or at a random point in the middle of the flight (value 0) (Coasting Start). To analyze the effect of the latitude and the number of satellites in view of a target, 8000 trajectories of a duration of 30 minutes each were randomly initialized in different global locations.

B. *Performance Analysis*

The performance of the proposed algorithm was measured in terms of distance at a given time between an estimated position and the known truth from the synthetically generated data. The error is measured as the great circle distance between the two positions and reported in Nautical Miles; the 95th, 98th, and 99th percentiles were computed for different aggregations, as described in the remainder of this section. Positions within the warmup period are not considered in this analysis.

1) Overall performance: Results highlighted corner cases, such as the initialization of the reference track at the reference system center (see III.D), which can be significantly far from the actual aircraft position and can drive the error to very high values if the warmup time expires before the track reaches a reasonable position. These corner cases will be addressed in future iterations of the algorithm by either filtering outliers in the solution or by modifications in the mathematical formulation or parameters used.

2) Performance by trajecotry type: In this analysis, trajectories are grouped by combinations of motion type, percentage of coasting, and coasting start. Fig. 3, Fig. 4, and Fig. 5 depict the results in terms of 95th, 98th, and 99th percentile of the error respectively. Motion types 1, 3, 5, and 6 report the worst performance, especially when looking at higher percentiles. The performance is greatly affected by the lack of position information at the beginning of the trajectory (Coasting Start = 1), which in most cases leads to the initialization of the track at the system center. The percentage of coasting causes a more gradual degradation of the performance, with significant decrease when the percentage is 100%, where no reported position information is available.

Fig. 3. Performance analysis per trajecotry type: 95th percentile error.

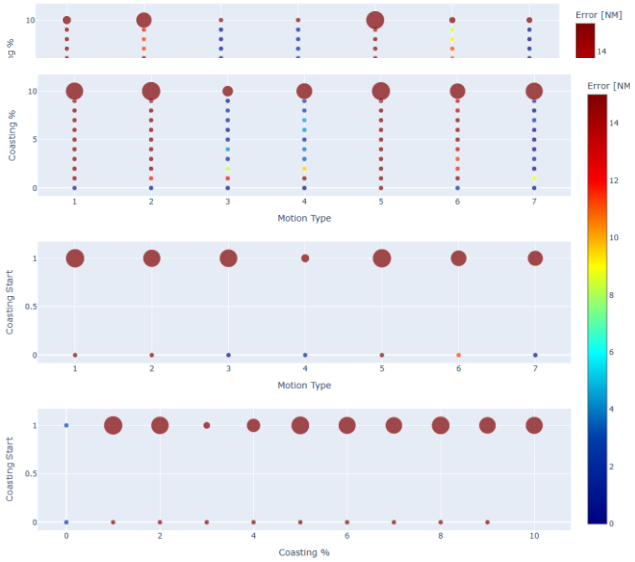

Fig. 4. Performance analysis per trajecotry type: 98th percentile error.

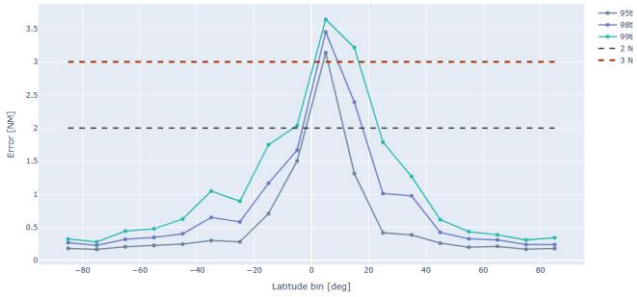

3) Performance by latitude: Another important driver of the performance for the proposed algorithm is the availability of TDOA opportunities, which requires reception of a message by two or more satellites. As described in [10], the probability of HPL footprint overlap decreases at lower latitudes (between -45 and 45 degrees). This trend is confirmed by the decrease in performance depicted in Fig. 6, Fig. 7, and Fig. 8 as a steep increase in the higher percentiles of the error between -45 and 45 degrees of latitude. Conversely, the 95th percentile of the error has a mild increase between -20 and 20 degrees. When looking at cases with low-to-moderate coasting percentage (less than or equal to 30% of the trajectory) for level flight at constant speed, which constitutes the vast majority of global trajectories, accelerations and decelerations , and climb/descent trajectories, it can be noticed how the performance are within the requriements of most surveillance and ATC systems, with the exception of very low latitudes (-15 to 15 degrees) for the climb descent motion type ().

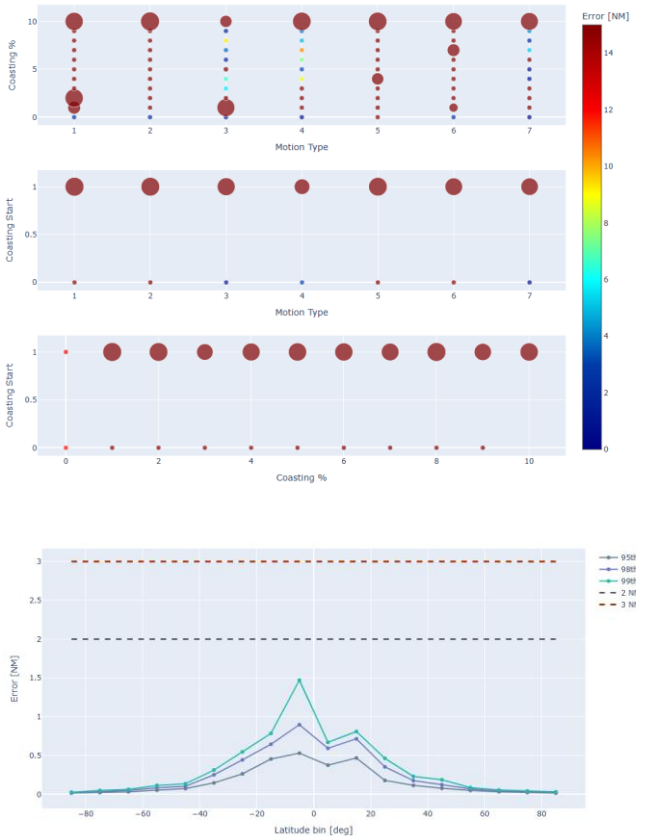

Fig. 5. Performance analysis per trajecotry type: 99th percentile error.

Fig. 6. Performance analysis by latitude – straight flight less than or equal to 50% coasting.

Fig. 7. Performance analysis by latitude – acceleration/deceleration less than or equal to 30% coasting.

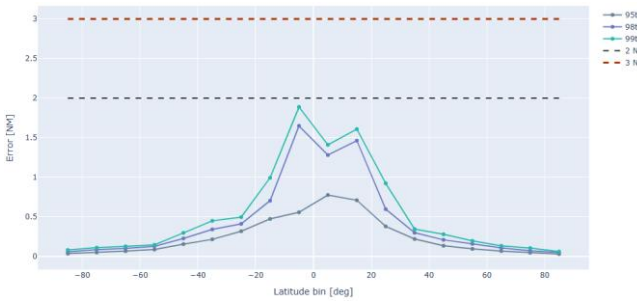

Fig. 8. Performance analysis by latitude – climb/descent less than or equal to 30% coasting.

V. Application to Real GNSS Anomalies

In this section, the proposed algorithm is applied to notable cases of aircraft affected by GNSS interference to showcase how RefTrack can be used to identify GNSS interference or to supplement other surveillance data when GNSS interference prevents the availability of position data.

Fig. 9. Flight UAE51N on 2024-05-09 - Independent estimation of position (green) vs reported ADS-B data (purple).

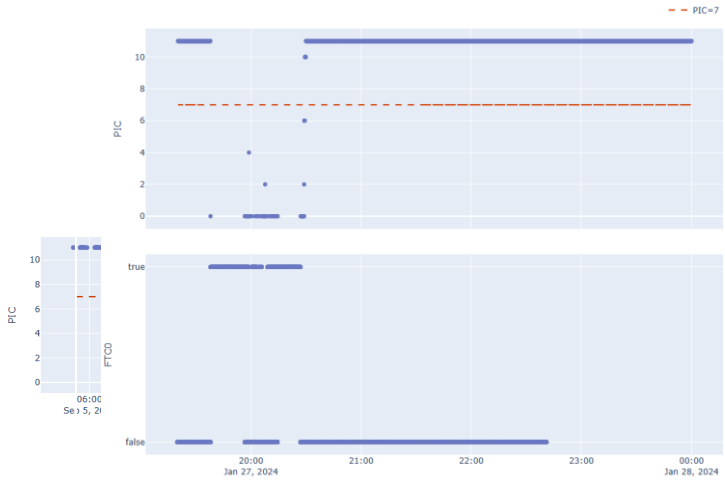

The first example is related to flight UAE51N on 2024-05-09, scheduled from Dubai DBX airport to San Francisco SFO airport. For the first portion of the flight, the aircraft reported position messages that followed a normal pattern for a commercial flight. After entering the Russian airspace, around 09:57Z, the aircraft started broadcasting positions that followed a sinusoidal pattern (Fig. 9) for the remainder of the flight, and that were characterized by a Position Integrity Category (PIC) 0, which means the estimated radius of containment for the position is > 20NM . Aireon's generated RefTrack in Fig. 9 shows the best estimate of the actual position of the aircraft. It can be noticed how the proposed algorithm correctly identifies the arrival position as being in San Francisco, albeit not terminating exactly at the airport.

Fig. 10. Flight UAE51N on 2024-05-09 – Timeline of the PIC.

The second example, flight CSC3816 on 2024-01-27 (Fig. 11) is a more classical case of GNSS interference where the aircraft started by emitting positions with degraded confidence, then it broadcasted Field Type Code 0 (FTC0) messages (Fig. 12) until it exits the GNSS interference region and recovers its GNSS capability. FTC0 messages are a special type of ADS-B message that the aircraft broadcasts when it loses the capability of resolving its GNSS position,. During the interference portion of the flight, the aircraft reported positions with high confidence in the Kazakhstan FIR, which were shown to air traffic controllers in the region, causing confusion as a "ghost" aircraft was appearing within their airspace.

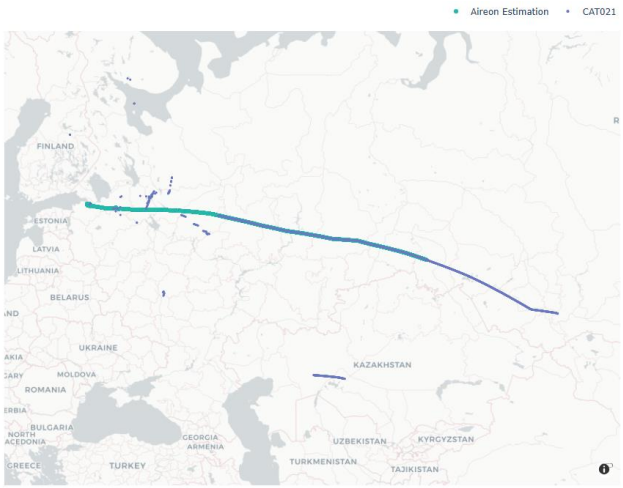

Fig. 11. Flight CSC3816 on 2024-01-27 - Independent estimation of position (green) vs reported ADS-B data (purple)

By computing the distance between the independently estimated position and the reported one, Aireon can flag unrealistic positions, thereby eliminating false track cases like the one in Kazakhstan.

One additional use case for the independent position estimation is filling gaps in information for air traffic stakeholders when the aircraft stops providing GNSS-based positions. That is the case of flight UAL163 operating between Dubai DBX and Newark EWR airports on 2024-11-16 (Fig. 13). The aircraft lost its GNSS capabilities 3 hours after take-off and it was not able to recover its position information for

Fig. 12. Flight CSC3816 on 2024-01-27 - Timeline of the PIC and FTC0 data.

Fig. 13. Flight UAL163 on 2024-11-16 - Independent estimation of position (green) vs reported ADS-B data (purple).

the remainder of the flight (Fig. 14). Aireon's innovative algorithm was able to estimate a reasonable route for the remaining 11.5 hours of flight, which crossed Europe, followed the North Atlantic routes, and terminated in the Newark area.

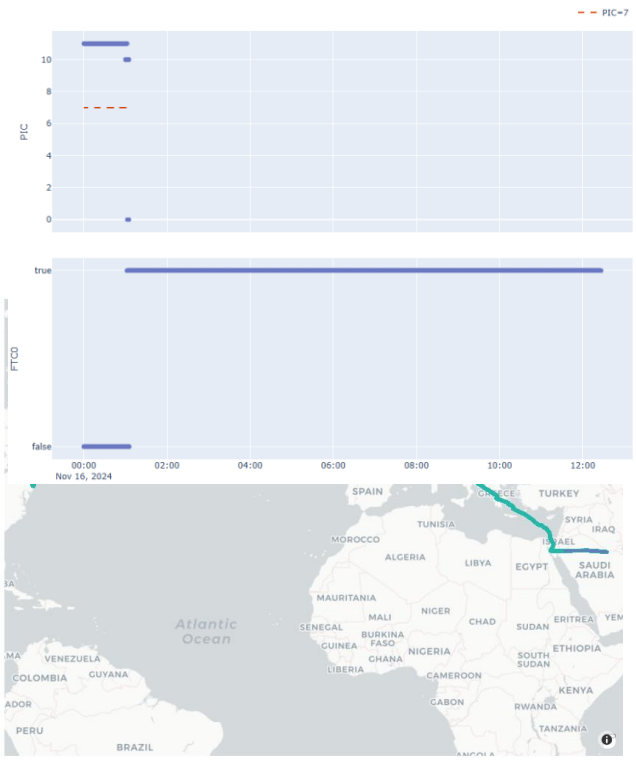

Fig. 14. Flight UAL163 on 2024-11-16 - Timeline of the PIC and FTC0 data.

This information would have been useful for the air traffic controllers monitoring the North Atlantic airspace: For big portions of the airspace, surveillance capability is solely based on ADS-B data, and as such, controllers rely on GNSS positions.

VI. Analysis of Teaffic Around Baku FIR

In order to assess the behavior of the proposed algorithm with real data, one hour of traffic within the region depicted in Fig. 15 was analyzed.

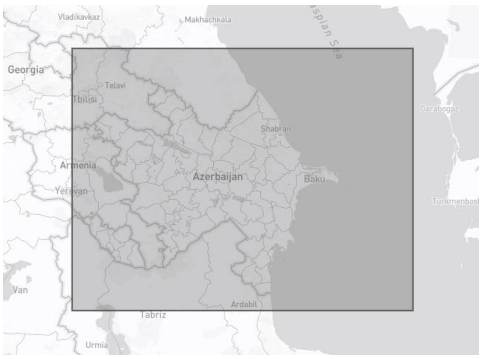

Fig. 15. Region around Baku FIR (UBBA) considered for analysis.

This region was chosen a it is surrounded by areas of known severe GNSS interference, thereby ensuring a mix of air traffic that enables the assessment of the algorithm against both aircraft that reported GNSS interference and aircraft that did not report any degradation. The time frame to investigate was chosen randomly as 2025-01-20 between 08:00Z and 08:59Z included. The dataset is comprised of 67 flights, 17 of which reported either a low PIC, a FTC0 message, or were flagged by Aireon's Independent Position Validation (IPV) [4].

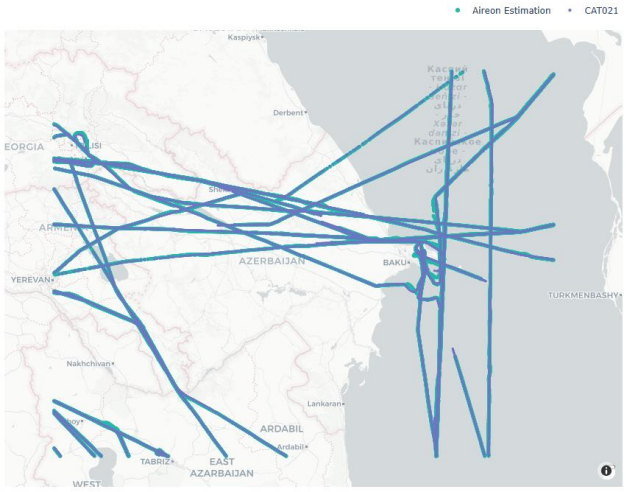

Fig. 16. Track relative to aircraft not affected by GNSS degradation. In green, Aireon's estimate and in purple, the reported ADS-B data.

The availability of tracks that are not affected by GNSS interference (Fig. 16) enables the computation of the accuracy of the results using the reported position as truth. The GNSS positons reported by each aircraft carry an associated accuracy, which can skew the error computations. By considering only positions with associated PIC ≥ 7, the radius of containment linked to each GNSS position is within 0.6NM, which, for the extent of this preliminary analysis, is considered negligible.

TABLE II. AGGREGATED PERFORMANCE RESULTS ACROSS NO GNSS DEGRADED FLIGHTS AROUND UBBA.

# Data Points	Error Percentile [NM]		
	95th	*98th*	*99th*
46,983	0.967	2.204	4.115

TABLE II. reports the aggregated error percentiles across all the datapoints generated for the flights not reporting any GNSS degradation in the timeframe considered. This performance is promising, however it must be considered that, with the exception of some turns, the vast majority of the tracks were reporting a straight flight pattern.

Fig. 17. Track relative to aircraft affected by GNSS degradation. In green

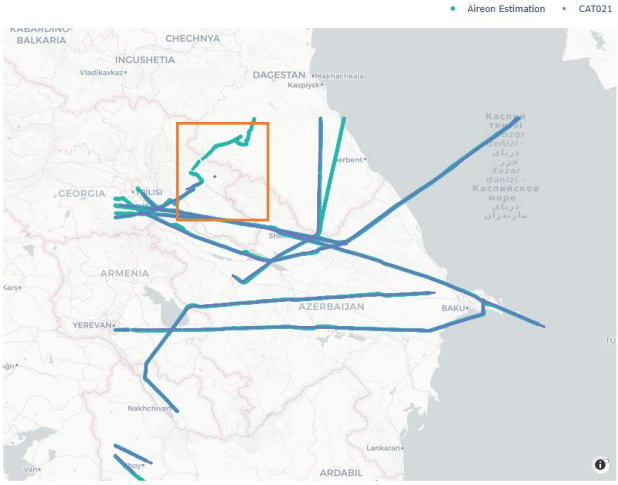

Aireon's estimate, and in purple, the reported ADS-B data.

The estimated positions for the flights that were affected by GNSS interference, depicted in Fig. 17, show that the algorithm performed generally well also when the reported information could not be trusted to power the prediction in the trackers. In cases such as the one highlighted in orange, the algorithm has difficulty keeping a steady trajectory due to lack of position information and disperse TDOA results.

Another important application of RefTrack output is the compensation of gaps in the CAT021 feed due to 1090MHz interference or to GNSS interference. TABLE III. presents the results of the Probability of Update (PoU) for a required Update Interval (UI) of 8s, computed following the methodology described in [15]. The output of Aireon position estimation algorithm provides an increase of around 4% in the PoU. In the current version of the algorithm, the generation of a track update is linked to the presence of ADS-B messages; however, the authors are exploring the possibility of updating the track even without the input of ADS-B messages, by exploiting the characteristics of the Kalman filters embedded in the algorithm, thereby increasing the resulting probability of update also in conditions of 1090 MHz interference.

TABLE III. PROBABILITY OF UPDATE FOR UPDATE INTERVAL OF 8S.

PoU(8s)	
CAT021	***RefTrack***
93.94%	97.82%

VII. CONCLUSION AND FUTURE WORK

GNSS interference is increasing at an unprecedented pace due to the geopolitical situation in several areas of the world and to the availability of more powerful and cheaper devices able to interfere with the GNSS spectrum. This degradation of the GNSS capability affects air traffic globally, with effects that expand beyond the areas of active interference.

This paper proposes an algorithm that enables the independent estimation of aircraft positions, which Aireon developed exploiting unique features of its systems. The

algorithm is still in its prototype stage, but preliminary results show promising performance when applied to diverse types of motion, albeit, in its current state, showing clear limitations on more complex maneuvers and when coasting persists for a long time. The paper also shows how this algorithm can be applied to the identification of GNSS interference and how it can complement surveillance sources when GNSS capabilities are degraded or absent.

Future work will focus on the fine-tuning of the parameters that affect the estimations, possibly moving from static to dynamic parameters that can adapt to the flight phase. Another improvement that the authors intend to investigate relates to the addition of constraints to the trackers to ensure that the estimations comply with aircraft capabilities and lie within the flight envelope.

ACKNOWLEDGMENT

The authors of this paper would like to thank Rafael Fraga, Joseph Canlas, and Joao de Castro Fortes for their support in the prototype implementation and the definition of the synthetic dataset. Furthermore, authors would like to thank Valerie Cox for her technical review and contributions to this paper.

REFERENCES

[1] M. A. Garcia, J. Dolan, G. Sirigu, "GPS interference and spoofing in the Baltics," 2024, [Online]. Available: https://aireon.com/white-paper-gps-interference-spoofing-in-the-baltics/

[2] IATA, "Global navigation satellite system GNSS radio frequency interference," 2024 [Online]. Available: https://www.iata.org/contentassets/c8e90fe690ce4047a8edfa97f4824890/iata_safety_risk_assessment_gnss_interference.pdf

[3] EASA, "Global navigation satellite system outage and alterations leading to communication / navigation / surveillance degradation," 2024 [Online]. Available: https://ad.easa.europa.eu/ad/2022-02R3

[4] J. Dolan and M. A. Garcia, "Aireon independent validation of aircraft position via space-based ADS-B," ESAVS, Berlin, 2018.

[5] P. Zarchan; H. Musoff. "Fundamentals of Kalman filtering: a practical approach." American Institute of Aeronautics and Astronautics, Incorporated, 2000. ISBN 978-1-56347-455-2

[6] D. Zhao, J. Sun and G. Gui, "En-route multilateration system based on ADS-B and TDOA/AOA for flight surveillance systems," *2020 IEEE 91st Vehicular Technology Conference (VTC2020-Spring)*, Antwerp, Belgium, 2020, pp. 1-6, DOI: 10.1109/VTC2020-Spring48590.2020.9129436.

[7] E. Widdison and D. G. Long, "A review of linear multilateration techniques and applications," IEEE Access, 2024.

[8] A. Norrdine, "An algebraic solution to the multilateration problem," Proceedings of the 15th international conference on indoor positioning and indoor navigation, Sydney, Australia, vol. 1315, 2012.

[9] Y. Zhou, L. Jun, and L. Lamont, "Multilateration localization in the presence of anchor location uncertainties," In 2012 IEEE Global Communications Conference (GLOBECOM), pp. 309-314 IEEE, 2012.

[10] J. Dolan, M. A. Garcia, and G. Sirigu, "Aireon Space Based Aircraft Position Validation And Multilateration Solution," *2023 IEEE/AIAA 42nd Digital Avionics Systems Conference (DASC)*, Barcelona, Spain, 2023, pp. 1-10, doi: 10.1109/DASC58513.2023.10311332.

[11] Aireon, "The executive reference guide to space-based ADS-B," McLean, 2020.

[12] M. A. Garcia, J. Dolan, B. Haber, A. Hoag, and D. Diekelman, "A compilation of measured ADS-B performance characteristics from Aireon's on-orbit test program," ESAVS, Berlin, 2018.

[13] J. Canlas, J. Dolan, and M. A. Garcia, "Update interval performance and outlier exclusion methods for aircraft surveillance systems," ICNS, Herndon, 2022.

[14] RTCA, "Minimum operational performance standards (MOPS) for 1090 MHz extended squitter automatic dependent surveillance – broadcast (ADS-B) and traffic information services – broadcast (TIS-B) ," 2011

[15] EUROCAE, "ED-129B - Technical Specification for a 1090 MHz Extended Squitter ADS-B Ground System", [Online]. Available: https://eshop.eurocae.net/eurocae-documents-and-reports/ed-129b/.